Fast Discrimination of Local Earthquakes Using a Neural Approach

by Flora Giudicepietro, Antonietta M. Esposito, and Patrizia Ricciolino

ABSTRACT

In this article, we describe a neural network method for the fast discrimination between local earthquakes and regional and teleseismic earthquakes using seismic records from a single station. Neural networks are data-driven nonlinear classifiers that learn from experience and can model real-world complex relationships. For the discrimination task, we implement a two-layer feed-forward multilayer perceptron (MLP). MLP is a supervised technique that accomplishes the learning process using a preclassified dataset for the training phase. The dataset includes 70 teleseisms, 79 regional earthquakes, and 103 local earthquakes. The seismic events are recorded at a single station, equipped with a short-period sensor. We parameterize the seismograms in the frequency domain, using the linear predictive coding (LPC). This technique is mostly used in audio signal processing for efficiently encoding frequency features of digital signals in a compressed form. The obtained spectral features, or LPC coefficients, are the input to the neural model. We carry out several tests by shortening from 4 to 1 s the time-window duration used for the LPC analysis. The proposed algorithm achieves a correct classification of 98.5% and 97.7% in discriminating local versus regional and local versus teleseismic earthquakes, respectively, on a 1-s time window. These results indicate that our discrimination algorithm can be profitably exploited in automatic analyses of seismic data that require fast responses, such as seismological monitoring systems and earthquake early warning systems.

INTRODUCTION

The problem of fast discrimination among different seismic events is crucial for timely communications to Civil Protection Authorities and to people exposed to natural hazards (earthquakes, tsunamis, volcanic eruptions, and floods). Current technology allows us to perform advanced automatic analysis to pick seismic phases (Allen, 1978; Rowe *et al.*, 2002; Lomax *et al.*, 2012), to locate earthquakes (Johnson *et al.*, 1995; Olivieri and Clinton, 2012), to estimate the shaking intensity in the area where the earthquake occurred (Wald *et al.*, 1999; Earle *et al.*, 2009), to locate volcanic seismic events (Wassermann and Ohrnberger, 2001; De Cesare *et al.*, 2009; Giudicepietro *et al.*, 2009; Olivieri and Clinton, 2012) and very long period events (Auger *et al.*, 2006), and to classify seismic events (Esposito, Giudicepietro, *et al.*, 2006; Langer *et al.*, 2006; Ochoa *et al.*, 2014; Kortström *et al.*, 2016; Mousavi *et al.*, 2016; Vargas *et al.*, 2016). A critical aspect of all of these advanced automatic analyses is a fast and robust recognition of seismic event types.

In recent decades, the scientific community has made considerable efforts to develop earthquake early warning (EEW) systems aimed at warning people, allowing them to take protective actions several seconds before the arrival of potentially damaging seismic waves (Basher, 2006; Böse *et al.*, 2008; Alcik *et al.*, 2009; Allen *et al.*, 2009; Zollo *et al.*, 2009, 2014; Given *et al.*, 2014). For these advanced seismic systems, too, the problem of a fast and robust seismic event discrimination is critical to avoid false alarms. For this reason, researchers have focused their attention on improving the robustness and reliability of fast automatic seismic analyses.

In this study, we deal with discrimination among teleseisms, regional earthquakes, and local earthquakes, according to the traditional seismogram classification based on the epicentral distance (Lay and Wallace, 1995). This discrimination is important because it allows us to recognize events that occurred outside the network of seismic stations, such as teleseismic and distant regional earthquakes, that are among the most common causes of failure of real-time earthquake systems (Lee and Stewart, 1981; Nakamura *et al.*, 2009; Li *et al.*, 2013; Zschau and Küppers, 2013, Zollo, 2016; Errata for Latest Earthquakes).

To this aim, we propose a neural classification of seismograms recorded at a single station that can be used, along with other methods based on the information produced by a seismic network of many stations (e.g., Earthworm, Johnson *et al.*, 1995), to attain a faster and more robust detection and classification of earthquakes. In recent years, artificial neural networks have been successfully used to approach seismic signal automatic classification (Wang and Teng, 1995; Falsaperla *et al.*, 1996; Ezin *et al.*, 2002; Avossa *et al.*, 2003; Scarpetta *et al.*, 2005; Esposito, Giudicepietro, *et al.*, 2006; Esposito, Scarpetta, *et al.*, 2006; Langer *et al.*, 2006; Esposito *et al.*, 2008; Esposito, D'Auria, Giudicepietro, Caputo, *et al.*, 2013; Horstmann *et al.*, 2013), and to detect events of particular interest (Del Pezzo *et al.*, 2003; Esposito, D'Auria, Giudicepietro, Caputo, *et al.*, 2013; Esposito, D'Auria, Giudicepietro, Peluso, *et al.*, 2013; Wiszniowski *et al.*, 2014). These techniques require a data preprocessing, aimed at feature extraction from seismograms, that typically exploits several seconds of the

doi: 10.1785/0220160222

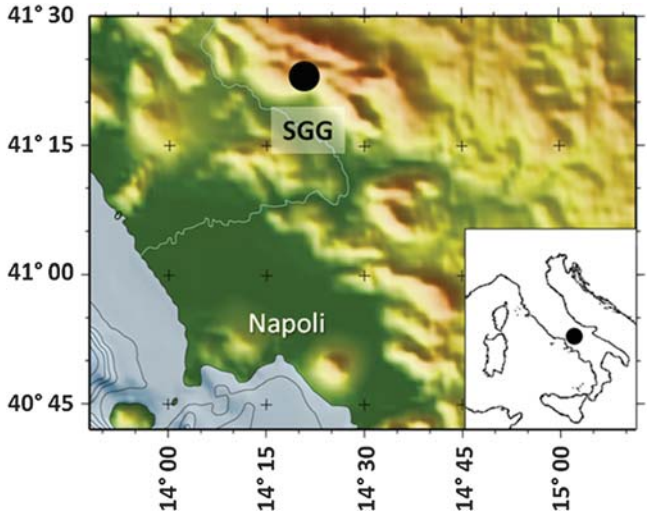

▲ **Figure 1.** Location of the SGG station.

seismic signal. The proposed neural analysis uses just a few seconds of the beginning of a seismogram to allow a fast discrimination among local, regional, and teleseismic earthquakes.

DATASET

Our dataset includes seismograms of local earthquakes, defined as earthquakes with an epicentral distance ≤100 km, of regional earthquakes with an epicentral distance of 100–1400 km, and of teleseisms with large epicentral distances ($\Delta \geq 30°$) (see Lay and Wallace, 1995). We use data from the SGG seismic station, operated by the Osservatorio Vesuviano (Istituto Nazionale di Geofisica e Vulcanologia [INGV]), that is located near San Gregorio Matese, a village situated in a seismically active area in the southern Apennines, Italy (Fig. 1). This station, equipped with a short-period sensor (Geotech S-13), has been operating since 1997. It has an analog system for data transmission. The data are then acquired by a 16-bit analog-to-digital (A/D) converter system. Our dataset includes 70 teleseisms and 79 regional earthquakes, recorded between 1999 and 2015, and 103 local earthquakes, most of which were recorded between 29 December 2013 and 30 January 2014 when a seismic swarm occurred in that area. Data are courtesy of the Osservatorio Vesuviano (INGV) seismic Lab (see Data and Resources). In our analysis, we use the vertical component. To apply a uniform automatic criterion for picking the onset of the seismic events, we exploit the ObsPy module for automatic *P*-phase picking (Withers *et al.*, 1998; Trnkoczy, 2012; Krischer *et al.*, 2015). In general, seismic automatic systems include specific modules for avoiding false triggers through the analysis of sets of automatic picking (e.g., the binder module in the Earthworm system, Johnson *et al.*, 1995; Zollo, 2016). For this reason, our data do not include false triggers, because their detection is beyond the scope of our analysis.

Figures 2 and 3 show examples of the three types of seismic events considered for the analysis, with the markers of the automatic picking. The teleseismic earthquakes recorded at

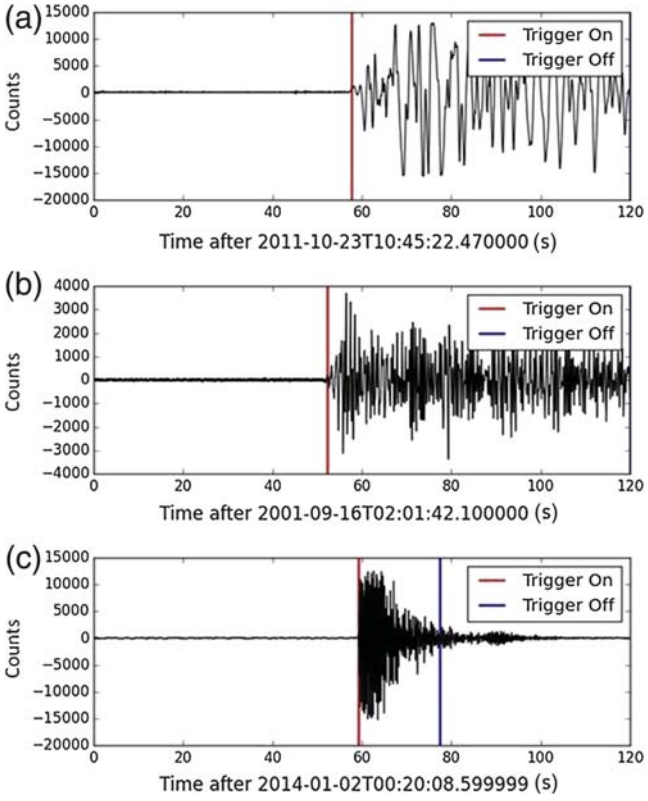

▲ **Figure 2.** Waveforms of (a) a teleseism, (b) a regional earthquake, and (c) a local earthquake. The red markers indicate the *P*-wave onset obtained using the ObsPy automatic picker. Blue marker indicates the trigger-off marker.

station SGG are characterized by a frequency range <3 Hz (Fig. 4). The regional earthquakes show higher frequency than the teleseismic ones (Fig. 4). The local earthquakes have typical waveforms, characterized by an impulsive onset, and are higher in frequency than the teleseisms and regional earthquakes (Figs. 2–4). Station SGG sometimes records earthquakes with magnitude greater than 3.5 that occurred at a small distance (<100 km). These events lead to the saturation of the seismic records and are not considered in this article.

ANALYSIS

For each event, we cut an initial data window of 20 s. The data sampling rate is 100 Hz. The starting point for the windows is the *P*-phase picking (Fig. 3). Next, we select smaller signal windows, with a variable length of 400, 200, and 100 samples, that is, from 4 to 1 s. We divide the time window of 400 samples (4 s) in two windows of 200 samples (2 s). Then, we apply the linear predictive coding (LPC) technique (Makhoul, 1975). This technique provides a compact data encoding that is suitable for reducing the input dimension to the neural network. In particular, the LPC models the signal spectrum in the frequency domain with an all-pole filter (Del Pezzo *et al.*, 2003) that compresses spectral information. In seismology, the spectrogram, based on the Fourier transform, is typically used

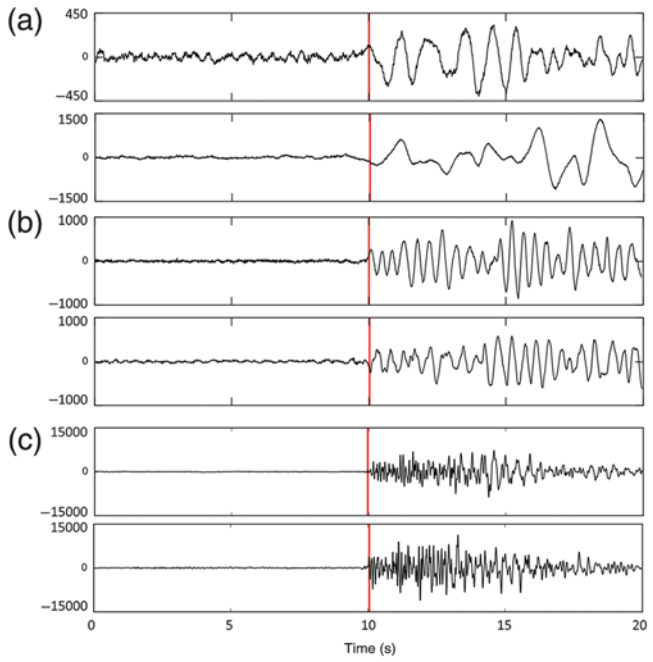

▲ **Figure 3.** Onset examples of (a) two teleseisms, (b) two regional earthquakes, and (c) two local earthquakes. The red markers indicate the *P*-wave onset obtained using the ObsPy automatic picker.

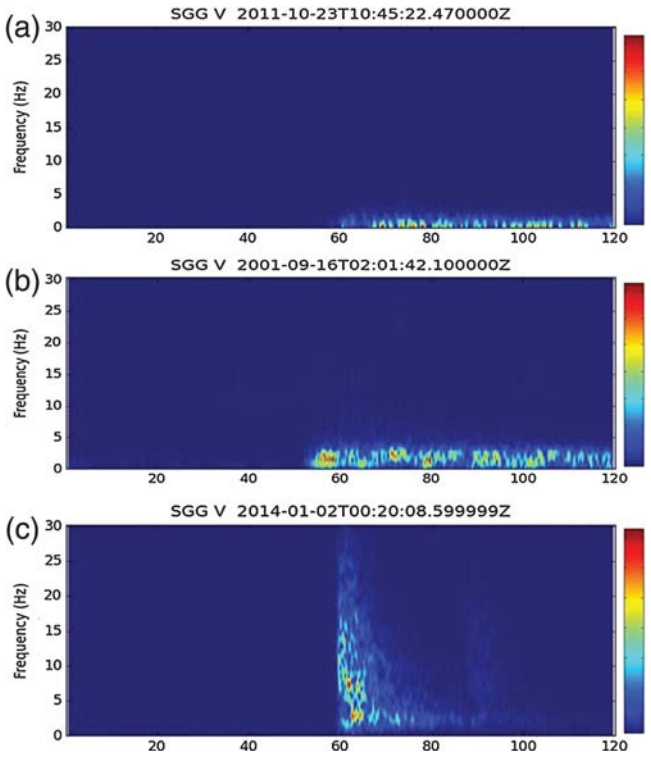

▲ **Figure 4.** Spectrograms of (a) a teleseism, (b) a regional earthquake, and (c) a local earthquake.

to characterize the signals, but it does not allow us to obtain a compact representation as input to the neural network. The linear prediction is a very efficient technique for eliminating correlation and redundancy from a signal. It is typically used in audio signal processing and speech analysis for representing the spectral envelope of a speech signal in a compact way. The LPC algorithm models each signal window, s_n, as a linear combination of its p previous samples as follows:

$$s_n^* = \sum_{k=1}^{p} c_k s_{n-k} + G, \tag{1}$$

in which s_n is the signal at time n, s_n^* is the LPC estimated or predicted signal, p is the model order that is problem-dependent, c_k, $k = 1, ..., p$, are the prediction coefficients, and G is the gain. The c_k estimation is obtained through a procedure that minimizes the error between the true signal and its LPC estimate. This procedure computes the following misfit function:

$$E(c) = \sum_n (s(n) - s^*(n))^2, \tag{2}$$

in which c is the vector of the c_k prediction coefficients. The c_k estimation is not time-consuming (Vaidyanathan, 2007), therefore it can be performed in real time.

In our experiments, we extract $p = 14$ coefficients for each signal window of 1 and 2 s (100 and 200 samples) to maximize the data compression and minimize the corresponding error. So, for each of these time windows, we obtain a vector of 14 spectral features (LPC coefficients). Furthermore, the time window of 4 s is divided in two subwindows of 2 s, and for each of them 14 LPC coefficients are extracted. So, the 4-s window is encoded by a vector of $14 + 14 = 28$ spectral features. Figures 5, 6, and 7 show the feature vectors obtained for signal windows of 1, 2, and 4 s, respectively.

METHOD

To discriminate among the different typologies of signals, we use a multilayer perceptron (MLP) network (Bishop, 1995; Haykin, 1999). MLP networks are neural supervised techniques, meaning that the learning process is realized by training the net on a prelabeled subset of data. The MLP architecture (Fig. 8) presents an input layer, one or more hidden layers, and an output layer. In our case, the input layer is the vector of the LPC coefficients computed for each signal, whereas the output layer provides the network response for each of the three examined classifications, that is, regional/local, teleseism/local, and teleseism/regional. There are neither intrastate nor feedback connections in the network, so the input signal $(x_1, ..., x_n)$ propagates from the input layer to the output one in a forward direction (i.e., feed forward). MLP networks have been widely used for function approximation, pattern classification, and recognition, due to their structural simplicity and fast learning abilities.

The dataset is divided into two subsets, one for training and the other one for testing the neural network. In particular,

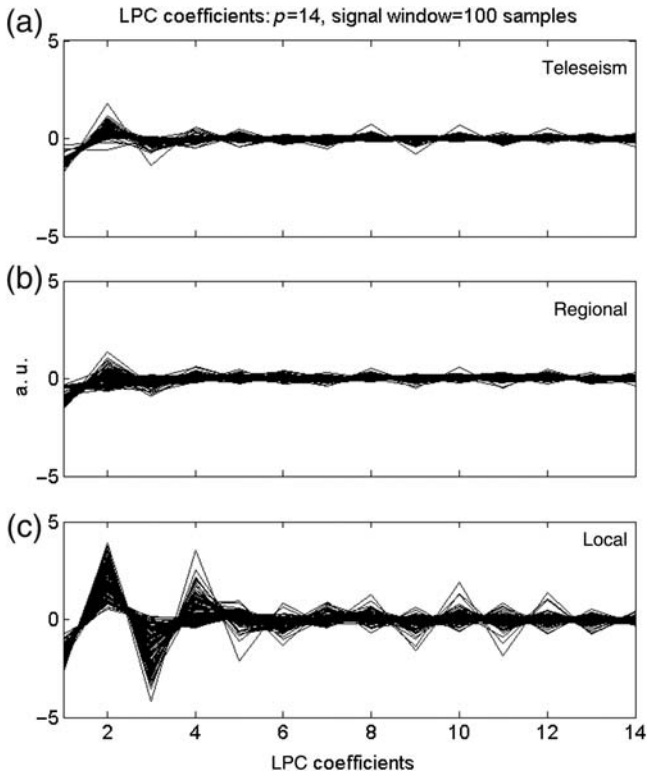

▲ **Figure 5.** Parameterization of 1 s of the seismic event onset. (a) Teleseisms, (b) regional earthquakes, and (c) local earthquakes.

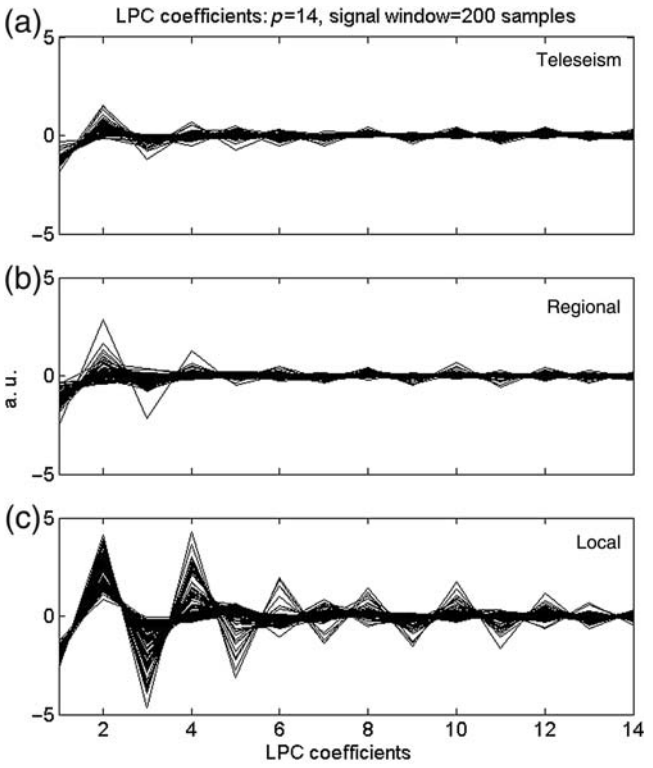

▲ **Figure 6.** Parameterization of 2 s of the seismic event onset. (a) Teleseisms, (b) regional earthquakes, and (c) local earthquakes.

we use 5/8 of the available dataset for the training phase and the remaining 3/8 for the testing one. In this way, the testing set is large enough to evaluate the network performance. Table 1 shows the adopted data distribution for the training and testing set in each classification task.

The setting of the net parameters (e.g., the initial weights on the connections, the number of hidden nodes, the activation functions, the learning algorithm, and the number of learning cycles) is tuned on the basis of previous works (Esposito, Scarpetta, *et al.*, 2006; Giudicepietro *et al.*, 2008; Esposito *et al.*, 2016). Moreover, we evaluate the final prediction error function as follows:

$$\mathrm{FPE} = s^2(p)\,\frac{N+p+1}{N-p-1} \tag{3}$$

(Akaike, 1970, 1974), in which N is the number of samples and $s^2(p)$ is the prediction error. $(N+p+1)/(N-p-1)$ increases with p and represents the inaccuracies in estimating the prediction parameters (Esposito, Scarpetta, *et al.*, 2006). We use a trial-and-error procedure to choose the appropriate number of LPC coefficients to represent the envelope of the signal spectrum in a compressed form (Fig. 9). Therefore, we use five hidden nodes for the MLP architecture and, as node activation functions, the hyperbolic tangent for the hidden units and the logistic sigmoidal for the output node.

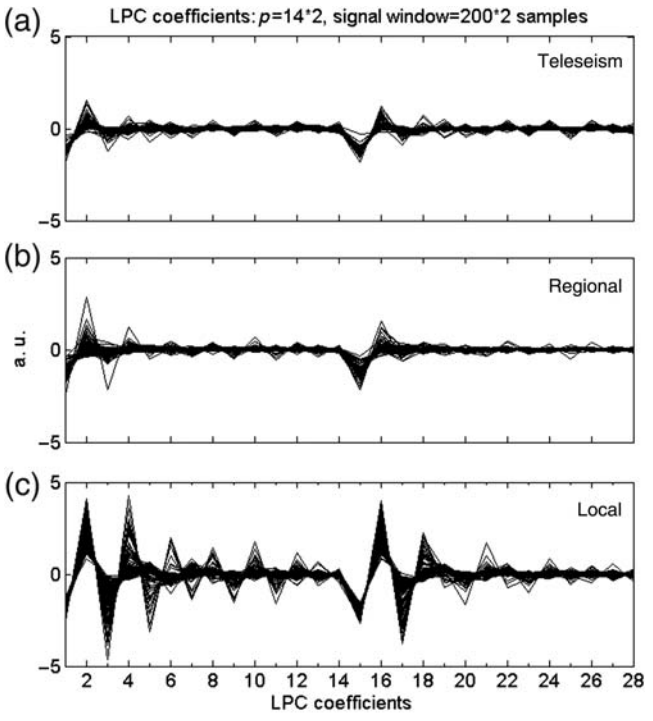

▲ **Figure 7.** Parameterization of 4 s of the seismic event onset. (a) Teleseisms, (b) regional earthquakes, and (c) local earthquakes.

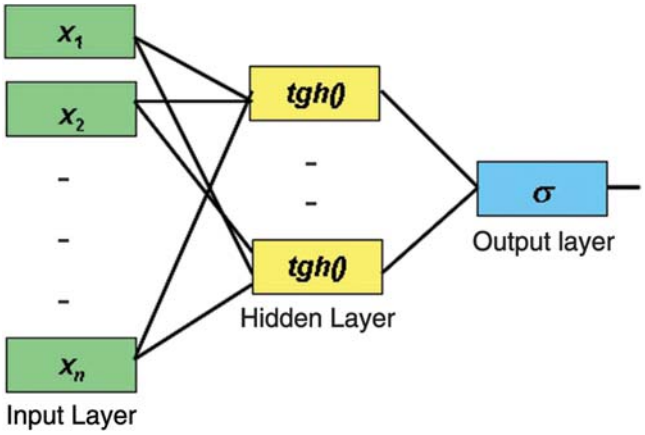

▲ **Figure 8.** An example of a two-layer multilayer perceptron (MLP) architecture. The input vector $(x_1, \ldots, x_n)$, that is, the linear predictive coding (LPC) coefficients, moves forward from the hidden layer to the output. There are no cycles and cross connections between the layers.

The quasi-Newton algorithm (Dennis and Schnabel, 1983; Bishop, 1995) is chosen for the weight optimization, and the cross-entropy error function (Bishop, 1995) is used as the error function for the output. The combined use of this algorithm with this function allows a probabilistic interpretation of the net response. We carry out 54 classification experiments, with a permutation of the training and testing subsets, to verify the stability of the network output, as described in the Results section.

The network training task takes less than 1 s on a PC with standard configuration. Once the network is trained, the recognition of a single event takes insignificant time (less than a hundredth of a second).

RESULTS

Table 2 summarizes the results of our analyses, showing the net performances for the three pairs of signals, namely, regional/local, teleseism/local, and teleseism/regional, for a total of 54 classification experiments. For each classification task (regional/local, teleseism/local, and teleseism/regional), we consider signal windows of the onset of the earthquakes with decreasing lengths (4, 2, and 1 s, respectively). Each row in Table 2 reports the net classification accuracy (in percentage) obtained on six different permutations of the training and testing sets and six random initial configurations of the net weights. Finally, the last column shows the average performance computed on each row. In Table 2, we can observe that good performances are obtained for the regional/local and the teleseism/local pair. In particular, an average of 98.53% of correct classification is achieved in the regional/local pair experiment, using only one second of the signal. For the teleseism/local pair, an average of 97.69% correct classification is obtained using one second of the signal and an average of 99.49% using the first four seconds of signal. The worst performance is that of the teleseism/regional pair, showing only 61% of correct classification on a one-second signal window. This performance increases up to 78.27% of correct classification when the first four seconds of the signal are considered, but it is still significantly lower than that obtained with the other two classification tasks (regional/local and teleseism/local). In our application, the short-period station introduces a high-pass filter on the signal, due to the instrumental response. For this reason, the regional earthquakes and the teleseisms are not sharply separated.

Table 1
Training and Testing Datasets Used for Each Type of Classification Task

Tasks	Training (5/8)	Testing (3/8)	Total
Regional/local	114	68	182
Teleseism/local	108	65	173
Regional/teleseism	93	56	149

CONCLUSIONS

The goal of this work is to provide a reliable neural network algorithm that works on signal windows as short as possible to allow an early identification of the different types of earthquakes and detect events outside the seismic network. In our case, the events outside the seismic network are regional and teleseismic earthquakes. The results of the proposed automatic neural classification are encouraging, because good performances are preserved on regional/local and teleseism/local classifications by shortening the signal window duration from 4 s up to 1 s. The method can be used with the signals of any short-period station; however, to achieve optimal performance, the neural network should be trained with examples of earthquakes recorded at that station, to realize a specialized detector (Scarpetta *et al.*, 2005). For broadband sensors, which ensure better quality of the teleseismic and regional seismograms, the spectral encoding does not allow very small time windows (e.g., window length $< T$, in which T is the period of the dominant components of the first P-wave arrival). However, we cannot exclude that, using other parameterization techniques (D'Auria *et al.*, 2006; Colombelli and Zollo, 2016), it is possible to overcome this problem.

In our experiments, we are able to discriminate between local and regional earthquakes, and local earthquakes and teleseisms, using only the first second of the seismograms, with a percentage of correct classification of 98.5% and 97.7%, respectively. The majority of local earthquakes belong to a seismic sequence that occurred between December 2013 and January 2014. Nonetheless, the neural network has also correctly classified the local earthquakes that do not belong to this seismic sequence. The seismic signal preprocessing is based on a speech signal-processing technique that allows effective data compres-

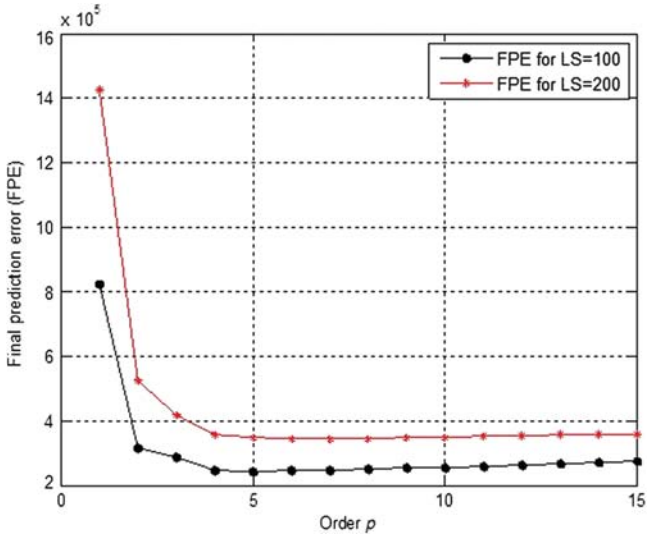

▲ **Figure 9.** Final prediction error (FPE) of the linear prediction coding evaluated for signal windows of 100 (black line) and 200 (red line) samples (1 and 2 s, respectively).

sion while maintaining the spectral information. Once the network is trained, the computation time for the classification is negligible. Therefore, we can obtain a robust discrimination on very short windows of the earthquake onset signal, in real time. The analysts typically recognize different types of seismic events through visual analysis of the waveforms. However, even the most experienced analysts can hardly distinguish in real time among the three examined types of events, just considering the first second of the seismograms.

This type of application of neural networks for the classification of seismic signals allows a profitable exploitation of old analog seismic stations that have the advantage of providing a large number of regional earthquake and teleseism recordings. This neural method, in conjunction with real-time earthquake analyses performed by advanced dense seismic networks, can improve the reliability of seismological monitoring systems. In particular, this technique can detect earthquakes that are located outside the seismic network. Furthermore, due to its very rapid response, the neural algorithm, with an appropriate tuning, can also be suitable for EEW systems to reduce the incidence of false alarms and the resulting erroneous communications to the public.

DATA AND RESOURCES

Seismograms used in this study were courtesy of Osservatorio Vesuviano–Istituto Nazionale di Geofisica e Vulcanologia, Italy (www.ov.ingv.it, last accessed May 2017). We used ObsPy system for the automatic picking of *P*-phase arrivals (www.obspy.org, last accessed April 2017)

ACKNOWLEDGMENTS

The authors thank the technical and technological staff that takes care of the seismic network and the seismic Laboratory at Osservatorio Vesuviano–Istituto Nazionale di Geofisica e Vulcanologia (INGV). The authors thank Anna Esposito and Novella Tedesco for their precious help with the English language improvements. Finally, the authors thank the reviewers and the editor who have helped improve this work.

Table 2
Multilayer Perceptron (MLP) Classification Performances

Earthquake (s; Npt; Input Nodes)	%Performance						Average
Regional/Local	**T1-1**	**T1-2**	**T1-3**	**T1-4**	**T1-5**	**T1-6**	
4 s; 400 samples; 28 input	98.52	100.00	100.00	100.00	97.05	98.52	99.02
2 s; 200 samples; 14 input	97.05	100.00	100.00	100.00	92.64	98.52	98.04
1 s; 100 samples; 14 input	98.52	97.05	100.00	100.00	95.58	100.00	98.53
Teleseism/Local	**T2-1**	**T2-2**	**T2-3**	**T2-4**	**T2-5**	**T2-6**	
4 s; 400 samples; 28 input	100.00	98.46	100.00	100.00	98.46	100.00	99.49
2 s; 200 samples; 14 input	100.00	98.46	96.92	96.92	98.46	96.92	97.95
1 s; 100 samples; 14 input	100.00	96.92	95.38	95.38	98.46	100.00	97.69
Regional/Teleseism	**T3-1**	**T3-2**	**T3-3**	**T3-4**	**T3-5**	**T3-6**	
4 s; 400 samples; 28 input	78.57	78.57	76.78	82.14	71.42	82.14	78.27
2 s; 200 samples; 14 input	73.21	75.00	71.42	71.42	71.42	67.85	71.72
1 s; 100 samples; 14 input	56.35	60.71	58.92	58.92	66.07	66.07	61.17

For each classification task, the first column reports the signal window duration in seconds (s), the corresponding number of samples (Npt), and the number of the neural network input nodes. We perform six different classification experiments for each window length, varying the set of events used for the network training and testing phase. We perform six permutations (1–6) of the training and testing datasets for each of the three classification tasks (T1, regional/local; T2, teleseism/local; T3, regional/teleseism). The last column reports the average performance value obtained on each signal length under examination.

REFERENCES

Akaike, H. (1970). Statistical predictor identification, *Ann. Inst. Statist. Math.* **22,** 202–217.

Akaike, H. (1974). A new look at the statistical model identification, *IEEE Trans. Automat. Contr.* **19,** 716–723.

Alcik, H., O. Ozel, N. Apaydin, and M. Erdik (2009). A study on warning algorithms for Istanbul earthquake early warning system, *Geophys. Res. Lett.* **36,** no. 5, doi: 10.1029/2008GL036659.

Allen, R. V. (1978). Automatic earthquake recognition and timing from single traces, *Bull. Seismol. Soc. Am.* **68,** 1521–1532.

Allen, R. M., P. Gasparini, O. Kamigaichi, and M. Böse (2009). The status of earthquake early warning around the world: An introductory overview, *Seismol. Res. Lett.* **80,** no. 5, 682–693, doi: 10.1785/gssrl.80.5.682.

Auger, E., L. D'Auria, M. Martini, B. Chouet, and P. Dawson (2006). Real-time monitoring and massive inversion of source parameters of very-long-period seismic signals: An application to Stromboli Volcano, Italy, *Geophys. Res. Lett.* **33,** L04301, doi: 10.1029/2005GL024703.

Avossa, C., F. Giudicepietro, M. Marinaro, and S. Scarpetta (2003). Supervised and unsupervised analysis applied to Strombolian E.Q., in *Neural Nets*, Springer, Berlin, Heidelberg, 173–178, doi: 10.1007/978-3-540-45216-4_19.

Basher, R. (2006). Global early warning systems for natural hazards: Systematic and people-centred, *Phil. Trans. Roy. Soc. Lond. A* **364,** no. 1845, 2167–2182, doi: 10.1098/rsta.2006.1819.

Bishop, C. (1995). *Neural Networks for Pattern Recognition*, Oxford University Press, New York, New York, 500 pp.

Böse, M., F. Wenzel, and M. Erdik (2008). PreSEIS: A neural network-based approach to earthquake early warning for finite faults, *Bull. Seismol. Soc. Am.* **98,** no. 1, 366–382, doi: 10.1785/0120070002.

Colombelli, S., and A. Zollo (2016). Rapid and reliable seismic source characterization in earthquake early warning systems: Current methodologies, results, and new perspectives, *J. Seismol.* **20,** no. 4, 1171–1186.

D'Auria, L., F. Giudicepietro, M. Martini, and R. Peluso (2006). Seismological insight into the kinematics of the 5 April 2003 vulcanian explosion at Stromboli volcano (southern Italy), *Geophys. Res. Lett.* **33,** no. 8, doi: 10.1029/2006GL026018.

De Cesare, W., M. Orazi, R. Peluso, G. Scarpato, A. Caputo, L. D'Auria, F. Giudicepietro, M. Martini, C. Buonocunto, M. Capello, *et al.* (2009). The broadband seismic network of Stromboli volcano, Italy, *Seismol. Res. Lett.* **80,** no. 3, 435–439, doi: 10.1785/gssrl.80.3.435.

Del Pezzo, E., A. Esposito, F. Giudicepietro, M. Marinaro, M. Martini, and S. Scarpetta (2003). Discrimination of earthquakes and underwater explosions using neural networks, *Bull. Seismol. Soc. Am.* **93,** no. 1, 215–223, doi: 10.1785/0120020005.

Dennis, J. E., and R. B. Schnabel (1983). *Numerical Methods for Unconstrained Optimization and Nonlinear Equations*, Prentice-Hall, Inc., Englewood Cliffs, New Jersey.

Earle, P. S., D. J. Wald, K. S. Jaiswal, T. I. Allen, K. D. Marano, A. J. Hotovec, M. G. Hearne, and J. M. Fee (2009). Prompt Assessment of Global Earthquakes for Response (PAGER): A system for rapidly determining the impact of global earthquakes worldwide, *U.S. Geol. Surv. Open-File Rept. 2009-1131*.

Esposito, A. M., L. D'Auria, F. Giudicepietro, T. Caputo, and M. Martini (2013). Neural analysis of seismic data: Applications to the monitoring of Mt. Vesuvius, *Ann. Geophys.* **56,** no. 4, doi: 10.4401/ag-6452.

Esposito, A. M., L. D'Auria, F. Giudicepietro, R. Peluso, and M. Martini (2013). Automatic recognition of landslides based on neural network analysis of seismic signals: An application to the monitoring of Stromboli volcano (southern Italy), *Pure Appl. Geophys.* **170,** no. 11, 1821–1832, doi: 10.1007/s00024-012-0614-1.

Esposito, A. M., F. Giudicepietro, L. D'Auria, S. Scarpetta, M. G. Martini, M. Coltelli, and M. Marinaro (2008). Unsupervised neural analysis of very-long-period events at Stromboli volcano using the self-organizing maps, *Bull. Seismol. Soc. Am.* **98,** no. 5, 2449–2459, doi: 10.1785/0120070110.

Esposito, A. M., F. Giudicepietro, S. Scarpetta, L. D'Auria, M. Marinaro, and M. Martini (2006). Automatic discrimination among landslide, explosion-quake, and microtremor seismic signals at Stromboli volcano using neural networks, *Bull. Seismol. Soc. Am.* **96,** no. 4A, 1230–1240, doi: 10.1785/0120050097.

Esposito, A. M., F. Giudicepietro, S. Scarpetta, and S. Khilnani (2016). A neural approach for hybrid events discrimination at Stromboli volcano, in *Multidisciplinary Approaches to Neural Computing*, Springer Series Smart Innovation, Systems and Technologies, Zurich, Switzerland.

Esposito, A. M., S. Scarpetta, F. Giudicepietro, S. Masiello, L. Pugliese, and A. Esposito (2006). Nonlinear exploratory data analysis applied to seismic signals, in *Neural Nets*, Springer, Berlin, Heidelberg, 70–77, doi: 10.1007/11731177_11.

Ezin, E. C., F. Giudicepietro, S. Petrosino, S. Scarpetta, and A. Vanacore (2002). Automatic discrimination of earthquakes and false events in seismological recording for volcanic monitoring, in *Neural Nets*, Springer, Berlin, Heidelberg, 140–145, doi: 10.1007/3-540-45808-5_15.

Falsaperla, S., S. Graziani, G. Nunnari, and S. Spampinato (1996). Automatic classification of volcanic earthquakes by using multi-layered neural networks, *Nat. Hazards* **13,** no. 3, 205–228.

Giudicepietro, F., L. D'Auria, M. Martini, T. Caputo, R. Peluso, W. De Cesare, M. Orazi, and G. Scarpato (2009). Changes in the VLP seismic source during the 2007 Stromboli eruption, *J. Volcanol. Geoth. Res.* **182,** no. 3, 162–171.

Giudicepietro, F., A. Esposito, L. D'Auria, M. Martini, and S. Scarpetta (2008). Automatic analysis of seismic data by using neural networks: Applications to Italian volcanoes, in *Conception, Verification, and Application of Innovative Techniques to Study Active Volcanoes*, W. Marzocchi and A. Zollo (Editors), Istituto Nazionale di Geofisica e Vulcanologia, Naples, Italy, 399–415.

Given, D. D., E. S. Cochran, T. Heaton, E. Hauksson, R. Allen, P. Hellweg, R. Vidale, and P. Bodin (2014). Technical implementation plan for the ShakeAlert production system: An earthquake early warning system for the west coast of the United States, *U.S. Geol. Surv. Open-File Rept. 2014-1097*, doi: 10.3133/ofr20141097.

Haykin, S. (1999). *Neural Networks: A Comprehensive Foundation*, Second Ed., Prentice-Hall, Englewood Cliffs, New Jersey.

Horstmann, T., R. M. Harrington, and E. S. Cochran (2013). Semiautomated tremor detection using a combined cross-correlation and neural network approach, *J. Geophys. Res.* **118,** no. 9, 4827–4846.

Johnson, C. E., A. Bittenbinder, B. Bogaert, L. Dietz, and W. Kohler (1995). Earthworm: A flexible approach to seismic network processing, *Incorporated Research Institutions for Seismology (IRIS) Newsletter*, **14,** no. 2, 1–4.

Kortström, J., M. Uski, and T. Tiira (2016). Automatic classification of seismic events within a regional seismograph network, *Comput. Geosci.* **87,** 22–30.

Krischer, L., T. Megies, R. Barsch, M. Beyreuther, T. Lecocq, C. Caudron, and J. Wassermann (2015). ObsPy: A bridge for seismology into the scientific Python ecosystem, *Comput. Sci. Dis.* **8,** no. 014003, doi: 10.1088/1749-4699/8/1/014003.

Langer, H., S. Falsaperla, T. Powell, and G. Thompson (2006). Automatic classification and *a-posteriori* analysis of seismic event identification at Soufriere Hills volcano, Montserrat, *J. Volcanol. Geoth. Res.* **153,** no. 1, 1–10, doi: 10.1016/j.jvolgeores.2005.08.012.

Lay, T., and T. C. Wallace (1995). *Modern Global Seismology*, Vol. 58, Academic Press, Cambridge, Massachusetts.

Lee, W. H. K., and S. W. Stewart (1981). *Principles and Applications of Microearthquake Networks*, Vol. 2, Academic Press, Cambridge, Massachusetts.

Li, J., X. Jin, H. Zhang, and Y. Wei (2013). Comparison of two earthquake early warning location methods, *Earthq. Sci.* **26,** no. 1, 15–22.

Lomax, A., C. Satriano, and M. Vassallo (2012). Automatic picker developments and optimization: FilterPicker—A robust, broadband picker for real-time seismic monitoring and earthquake early warning, *Seismol. Res. Lett.* **83,** no. 3, 531–540, doi: 10.1785/gssrl.83.3.531.

Makhoul, T. (1975). Linear prediction: A tutorial review, *Proc. IEEE* **63,** no. 4, 561–580.

Mousavi, S. M., P. H. Stephen, C. A. Langston, and B. Samei (2016). Seismic features and automatic discrimination of deep and shallow induced-microearthquakes using neural network and logistic regression, *Geophys. J. Int.* **207,** 29–46, doi: 10.1093/gji/ggw258.

Nakamura, H., S. Horiuchi, C. Wu, S. Yamamoto, and P. A. Rydelek (2009). Evaluation of the real-time earthquake information system in Japan, *Geophys. Res. Lett.* **36,** no. 5, doi: 10.1029/2008GL036470.

Ochoa, L. H., L. F. Niño, and C. A. Vargas (2014). Severity classification of a seismic event based on the magnitude–distance ratio using only one seismological station, *Earth Sci. Res. J.* **18,** no. 2, 115–122.

Olivieri, M., and J. Clinton (2012). An almost fair comparison between Earthworm and SeisComp3, *Seismol. Res. Lett.* **83,** no. 4, 720–727.

Rowe, C. A., R. C. Aster, B. Borchers, and C. J. Young (2002). An automatic, adaptive algorithm for refining phase picks in large seismic data sets, *Bull. Seismol. Soc. Am.* **92,** no. 5, 1660–1674, doi: 10.1785/0120010224.

Scarpetta, S., F. Giudicepietro, E. C. Ezin, S. Petrosino, E. Del Pezzo, M. Martini, and M. Marinaro (2005). Automatic classification of seismic signals at Mt. Vesuvius volcano, Italy, using neural networks, *Bull. Seismol. Soc. Am.* **95,** no. 1, 185–196, doi: 10.1785/0120030075.

Trnkoczy, A. (2012). Understanding and parameter setting of STA/LTA trigger algorithm, in *New Manual of Seismological Observatory Practice 2 (NMSOP-2)*, IS 8.1, Deutsches GeoForschungsZentrum GFZ, Potsdam, Germany, 20 pp.

Vaidyanathan, P. P. (2007). The theory of linear prediction, *Synth. Lect. Signal Process.* **2,** no. 1, 1–184.

Vargas, M. G., J. Rueda, R. M. G. Blanco, and J. Mezcua (2016). A real-time discrimination system of earthquakes and explosions for the mainland Spanish seismic network, *Pure Appl. Geophys.* **174,** 1–16, doi: 10.1007/s00024-016-1330-z.

Wald, D. J., V. Quitoriano, T. H. Heaton, H. Kanamori, C. W. Scrivner, and C. B. Worden (1999). TriNet "ShakeMaps": Rapid generation of peak ground motion and intensity maps for earthquakes in southern California, *Earthq. Spectra* **15,** no. 3, 537–555.

Wang, J., and T. L. Teng (1995). Artificial neural network-based seismic detector, *Bull. Seismol. Soc. Am.* **85,** no. 1, 308–319.

Wassermann, J., and M. Ohrnberger (2001). Automatic hypocenter determination of volcano induced seismic transients based on wavefield coherence—An application to the 1998 eruption of Mt. Merapi, Indonesia, *J. Volcanol. Geoth. Res.* **110,** no. 1, 57–77, doi: 10.1016/S0377-0273(01)00200-1.

Wiszniowski, J., B. Plesiewicz, and J. Trojanowski (2014). Application of real time recurrent neural network for detection of small natural earthquakes in Poland, *Acta Geophys.* **62,** no. 3, 469–485, doi: 10.2478/s11600-013-0140-2.

Withers, M., R. Aster, C. Young, J. Beiriger, M. Harris, S. Moore, and J. Trujillo (1998). A comparison of select trigger algorithms for automated global seismic phase and event detection, *Bull. Seismol. Soc. Am.* **88,** no. 1, 95–106.

Zollo, A. (2016). A new tool for rapid and automatic estimation of earthquake source parameters and generation of seismic bulletins, presented at the *EGU General Assembly Conference Abstracts*, Vol. 18, 15,638.

Zollo, A., S. Colombelli, L. Elia, A. Emolo, G. Festa, G. Iannaccone, C. Martino, and P. Gasparini (2014). An integrated regional and on-site earthquake early warning system for southern Italy: Concepts, methodologies and performances, in *Early Warning for Geological Disasters*, Advanced Technologies in Earth Sciences, Springer, Berlin, Heidelberg, 117–137, doi: 10.1007/978-3-642-12233-0_7.

Zollo, A., G. Iannaccone, M. Lancieri, L. Cantore, V. Convertito, A. Emolo, G. Festa, F. Gallovič, M. Vassallo, C. Martino, *et al.* (2009). Earthquake early warning system in southern Italy: Methodologies and performance evaluation, *Geophys. Res. Lett.* **36,** L00B07, doi: 10.1029/2008GL036689.

Zschau, J. and A. N. Küppers (Editors) (2013). *Early Warning Systems for Natural Disaster Reduction*, Springer Science & Business Media, New York, New York.

Flora Giudicepietro
Antonietta M. Esposito
Patrizia Ricciolino
Istituto Nazionale di Geofisica e Vulcanologia
Osservatorio Vesuviano
via Diocleziano 328
80124 Naples, Italy
flora.giudicepietro@ingv.it
antonietta.esposito@ingv.it
patrizia.ricciolino@ingv.it

Published Online 31 May 2017